

# Journal of Intelligent Material Systems and Structures

<http://jim.sagepub.com/>

---

## Tailored Current—Voltage Relationships of Droplet-Interface Bilayers Using Biomolecules and External Feedback Control

Stephen A. Sarles and Donald J. Leo

*Journal of Intelligent Material Systems and Structures* 2009 20: 1233 originally published online 27 April 2009

DOI: 10.1177/1045389X09104390

The online version of this article can be found at:

<http://jim.sagepub.com/content/20/10/1233>

---

Published by:



<http://www.sagepublications.com>

Additional services and information for *Journal of Intelligent Material Systems and Structures* can be found at:

**Email Alerts:** <http://jim.sagepub.com/cgi/alerts>

**Subscriptions:** <http://jim.sagepub.com/subscriptions>

**Reprints:** <http://www.sagepub.com/journalsReprints.nav>

**Permissions:** <http://www.sagepub.com/journalsPermissions.nav>

**Citations:** <http://jim.sagepub.com/content/20/10/1233.refs.html>

>> [Version of Record](#) - Jun 10, 2009

[Proof](#) - Apr 27, 2009

[What is This?](#)

# Tailored Current–Voltage Relationships of Droplet-Interface Bilayers Using Biomolecules and External Feedback Control

STEPHEN A. SARLES\* AND DONALD J. LEO

*Center for Intelligent Material Systems and Structures, Dept. of Mechanical Engineering  
Virginia Tech, 310 Durham Hall, Blacksburg, VA 24061, USA*

**ABSTRACT:** The development of a new class of active material based on the ion transport properties of functional biomolecules is introduced in this work. The new class of materials utilizes a recently developed technique known as the droplet-interface bilayer (DIB) to enable the reconstitution of biomolecules into a durable matrix. Methods to modify the current–voltage relationship across the bilayer, including the incorporation of proteins and the use of an external feedback loop, are explored. Electrical impedance spectroscopy and cyclic voltammetry measurements are used to characterize the bilayers and indicate that a single DIB can be modeled as a resistor in parallel with a capacitor. Alpha-hemolysin proteins from *Staphylococcus aureus* cause a reduction in the resistance of the bilayer and exhibit current-rectification at positive *cis* potentials. Alamethicin proteins from *Trichoderma viride* produce a voltage-dependent conductance allowing the specific resistance ( $M\Omega\text{cm}^2$ ) of the bilayer to be varied reversibly by 2–3 orders of magnitude. Feedback integral current control is demonstrated on pure 1,2-diphytanoyl-sn-glycero-3-phosphocholine DIBs and provides accurate current tracking at a driving rate of 10 mHz and less. Proportional–integral voltage control applied to a DIB establishes a second-order frequency response where the natural frequency and damping ratio of the resonance can be selected.

*Key Words:* biomolecular networks, droplet-interface bilayer (DIB), bilayer lipid membrane (BLM), electrical impedance spectroscopy (EIS), cyclic voltammetry (CV), alpha-hemolysin, alamethicin, feedback control, current–voltage relationship.

## INTRODUCTION

THE relationship between the transport and separation of charges define the operating characteristics of many active materials, including the arrangement of electric dipoles in piezoelectric ceramics, the accumulation of mobile cations in ionic polymer transducers (IPTs) (Duncan et al., 2008), and the gating characteristics of novel transistors (Bernards et al., 2006). In the cellular structures of plants and animals, the distribution and transfer of charges is similarly defined by the motions of mobile ions (Evans et al., 1991; de Angeli et al., 2007). The movement of these ions is bounded by phospholipid membranes that act as physical barriers to inorganic ions and water molecules and that define the outer boundaries and internal regions of a cell (Tien and Ottova, 2001). Biological molecules such as proteins and ion channels residing in these lipid membranes provide selective pathways for ion flow through the lipid membranes, enabling the active functionality of the

cell structure including sensing, actuation, and regulation of metabolic tasks. Proteins and ion channels derived from natural sources offer a highly diverse array of functionality – some act as enzymes required to carry out chemical reactions (Lewis et al., 2006), others function as active ion pumps (Lanyi and Pohorille, 2001), and still others act as energy-conversion molecules (Luo et al., 2005).

Recently, interest in using biological molecules such as phospholipids, proteins, and ion channels has led to the development of several types of bio-inspired materials and devices: chemical sensors (Nikolelis and Sintonrou, 1995; Schmidt et al., 2000; Castellana and Cremer, 2006; Reimhult and Kumar, 2008), rotary motors (Hess and Vogel, 2001; Rondelez et al., 2005), and bio-transistors (Bernards et al., 2006). In most of these works, proteins or ion channels are the active elements and were reconstituted into an artificial bilayer lipid membrane (BLM). Sundaresan et al. (2007a) and Sundaresan and Leo (2008) used ATPase enzymes and SUT4 proteins reconstituted into bilayer lipid membranes in order to move sucrose and water across lipid membranes formed across the pores of a porous

\*Author to whom correspondence should be addressed.  
E-mail: sarles@vt.edu; andysarles@hotmail.com  
Figures 1–11 and A1 appear in color online: <http://jim.sagepub.com>

support—creating a chemomechanical, protein-powered pump. The ATPase enzymes hydrolyze available adenosine triphosphate (ATP), establishing a pH gradient across the membrane used to trigger the SUT4 proteins. A second device concept relying on reconstituted proteins to emerge from this work used ATPase enzymes alone to convert chemical energy in the form of ATP into electricity that was sourced to an external circuit (Sundaresan et al., 2007b). The Biocell – as it is named – produced  $1\text{--}2\ \mu\text{W}/\text{cm}^2$  of lipid membrane and per  $15\ \mu\text{L}$  of ATPase enzyme added to the system.

In this article, we present results that enable the development of a new class of smart material that utilizes the transport properties of biomolecules as the transduction mechanism. Our work is inspired by the fact that biological networks utilize charge and mass transport as a means of producing very complex functions such as cell signaling, system regulation, tissue regeneration, and healing. The ultimate goal of our work is to utilize similar physical processes to engineer a new class of durable material that can be tailored to provide novel types of stimulus-responsive behavior in material systems. As shown in Figure 1, the types of stimulus-responsive behavior we are envisioning consist of responses to common physical stimuli such as sound, force, heat, and light. As is the case for biological systems, our new biologically inspired materials will utilize the transport properties of biomolecular networks to create complex input–output relationships that lead to new types of functional behaviors in materials. In this manner, we will create a truly hierarchical system that utilizes the properties of materials and the activities of biomolecules at very small length scales to enable complex system behaviors at larger length scales.

The building block of this new type of material system can be thought of as an ‘artificial cell’ that consists of an aqueous medium surrounded by biomolecules that

enable the cell to be interfaced with other cells in the network. The ‘cells’ are investigated by measuring the current–voltage relationship of ions across lipid bilayers formed from droplet-interface bilayers (DIBs) – a recently developed technique for bilayer formation. We demonstrate that biological molecules and, for the first time, external feedback control can be used to tailor the ion transport properties of lipid membranes and that this authority can be used to develop new active, controllable biosystems formed from DIBs. Electrical impedance spectroscopy (EIS) and cyclic voltammetry (CV) measurements are used to characterize the electrical properties, namely the current–voltage relationship, of bilayer lipid membranes both with and without proteins. Alpha-hemolysin ( $\alpha\text{HL}$ ) from *Staphylococcus aureus* and alamethicin from the fungus *Trichoderma viride* reconstituted into the BLMs provide convenient methods for modifying the selectivity of the lipid membranes and altering the current–voltage relationships. Feedback control is applied in two different fashions in order to customize the transport dynamics of the BLMs for both current tracking and voltage control.

## METHODOLOGIES OF BILAYER FORMATION

A common requirement for investigating and assembling protein-powered device concepts is the formation of a bilayer (or ‘black’) lipid membrane (BLM) (Mueller et al., 1962; Haydon and Taylor, 1963; Tien and Ottova, 2001; Ottova and Tien, 2002). A BLM, or lipid bilayer, consists of amphiphilic phospholipid molecules that self-assemble in water into either planar BLMs or spherical BLMs (called liposomes) in order to minimize free energy (Gruen and Haydon, 1981; Needham and Haydon, 1983). This 5–7 nm thick artificial phospholipid membrane (Figure 2(a)) mimics

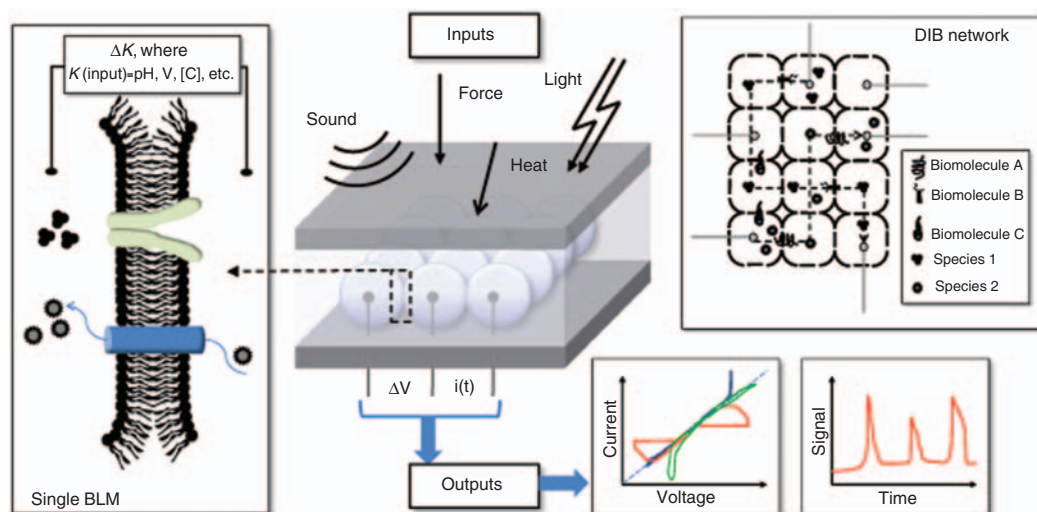


**Figure 1.** Active materials that utilize the transport properties of biomolecules are constructed from networks of DIBs. Proteins incorporated into specific bilayer interfaces in the network determine the input/output transduction relationship to multiple stimuli.

those found in cells and provides a suitable environment for the reconstitution of proteins (Mueller et al., 1962, 1964; Hladky and Haydon, 1970, 1972; Sackmann, 1996; Ottova and Ti Tien, 1997; Tien and Ottova, 2001). The term ‘black lipid membrane’ first emerged from observations of soap films at the air–water interface performed by Robert Hooke and Isaac Newton in the 17th century (Tien and Ottova, 2001) and then was later coined in relation to lipid films by Mueller et al. (1962). These researchers observed that the mono- and bi-layer molecular films formed from soap and lipid molecules, respectively, did not reflect incident light due to their ultra-thin structures, thus having a ‘black’ appearance. The formation and characterization of artificial BLMs has been extensively researched for nearly 50 years and, in a great majority of these works, planar lipid bilayers have been formed across the pore(s) of a synthetic substrate in water using methods such as lipid folding or painting or by the use of a feeder tube (Requena et al., 1975). This configuration offers convenient access to both sides of the membrane for making electrical measurements of the lipid bilayer (Mueller et al., 1962; Haydon and Taylor, 1963; Mueller and Rudin, 1963; Hanai et al., 1964, 1965; Tien, 1984; Sabo et al., 1997; Wiegand et al., 2002; Naumowicz, Petelska and Figaszewski, 2003, 2005; Sarles et al., 2007) and for studying the functions of proteins or ion channels within the membrane (Hladky and Haydon, 1970, 1972; Andersen, 1983; Menestrina, 1986; Cheng et al., 2001; Naumann et al., 2002). This technique, however, is limited by the fragility of the membrane and demands great attention to the geometry and surface chemistry of the supporting substrate, which can complicate BLM formation. Moreover, traditional supported and suspended BLMs formed on gold, porous alumina, and Teflon substrates (Lauger et al., 1967; Montal and Mueller, 1972; Thompson et al., 1982; Nikolelis and Siontorou, 1995; Schmidt et al., 2000; Romer and Steinem, 2004) are difficult to assemble into higher order systems where the functionality is based on the inherent activity and function of the proteins.

The DIB method is a technique for forming durable bilayer lipid membranes that eliminates the need for supporting substrates (Figure 2(b)). Funakoshi et al. (2006) first attempted this technique as initial validation that intersecting aqueous and lipid solution streams could be used to form BLMs within micro-fluidic channels. Holden et al. (2007) refined and expanded the approach to demonstrate that this technique produces BLMs that last for days and that the droplets can be arranged and rearranged to form stable networks of nanoliter-volume water droplets interconnected by DIBs (Holden, Needham and Bayley, 2007). Biological networks created from DIBs enable the development of active systems based on inherent molecular functionality. By tailoring the contents of each droplet as well as the relative placement of adjacent droplets, the DIB method also provides a novel test-bed for studying complex interactions between biological components, conducting controlled reactions within nanoliter volumes, and creating functional networks using biologically inspired molecules. We believe that prospective applications for these modular networks include energy harvesting, chemical and/or bio-data storage, and sensing.

## EXPERIMENTAL METHODS

DIBs are formed (Figure 3) using the procedures developed by Holden et al. (Hanai et al., 1965; Haydon and Taylor, 1963). The aqueous droplets contain 10 mM MOPS (4-Morpholinepropanesulfonic acid, Sigma), 100 mM NaCl (sodium chloride, Sigma), pH 7 buffer solution. 1,2-diphytanoyl-sn-glycero-3-phosphocholine (DPhPC) synthetic lipids purchased as lyophilized powder (Avanti Polar Lipids, Inc.) are dissolved in hexadecane (Sigma) to form a 10 mg/mL lipid stock solution. First, a well machined into a poly(methyl methacrylate) (PMMA) tray is filled with lipid solution (Figure 3). Then, two droplets of buffer solution are injected into the lipid solution and positioned such that

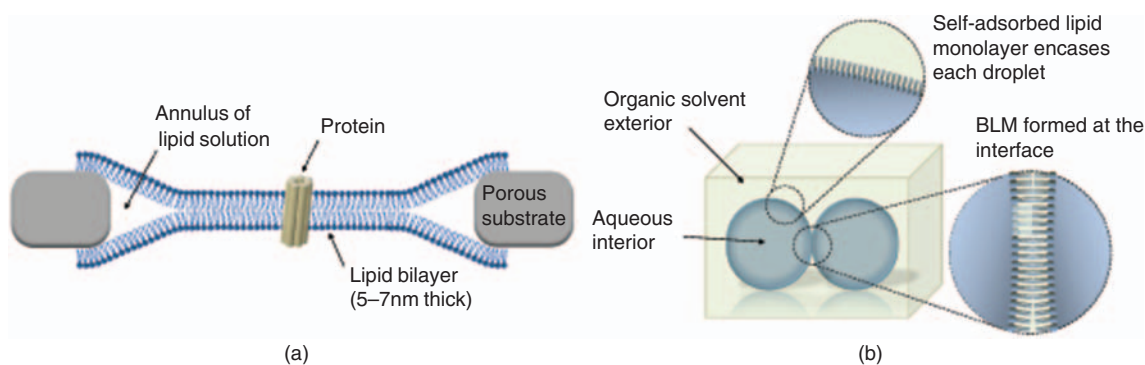


**Figure 2.** Cross-sectional views of a suspended bilayer lipid membrane formed within the pore of a porous support (a) and a DIB formed at the interface of two lipid-encased water droplets surrounded by a lipid/organic solvent solution (b). Typical solvents used in bilayer formation include squalene, decane, and hexadecane.

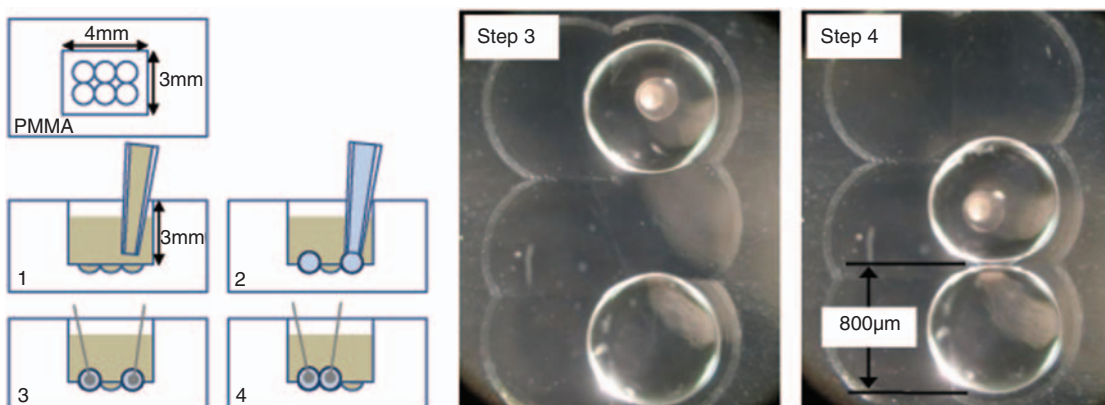


**Figure 3.** DIBs are formed when water droplets (300 nL each) are pipetted (2) into lipid solution within a well (1). After several hours to allow for lipid monolayer assembly at the oil/water interface around each droplet (3), the two droplets are pierced with agarose-tipped Ag/AgCl electrodes and brought together in contact (4). The interface bilayer forms when excess organic solvent is extracted from between the droplets and the two lipid monolayers 'zip' together.

they are not touching. The amphiphilic lipid molecules from the surrounding lipid solution migrate and assemble at the oil/water interface (Lee et al., 2001). Holden et al. (2007) found that DIBs could be produced repeatedly when the monolayers were allowed to 'stabilize' for 30 min (Holden, Needham and Bayley, 2007); however, our results indicate several hours are needed to establish stable interfacial membranes from well-packed lipid monolayers when using DPhPC phospholipids (with a gel-to-fluid transition temperature of 41°C) dissolved in hexadecane at room temperature. A silver–silver chloride electrode coated with agarose gel (Sigma) is then inserted by hand into each droplet, and following an additional 10–20 min for the monolayers to re-stabilize, the electrodes are positioned in order for the droplets to come into contact (Holden, Needham and Bayley, 2007). More complex networks of DIBs can be made by connecting additional droplets.

EIS and CV are used to characterize the electrical properties of DIBs with and without proteins. An Autolab PGSTAT12 (Eco Chemie) Potentiostat/Galvanostat with a FRA2 module and controlled by FRA and GPES software is used to perform these tests. Electrical impedance measurements of the DIBs are performed using a 5 mV (RMS) sinusoidal potential swept from 500 kHz to 0.01 Hz. CV measurements are conducted with a scan rate of 1 mV/s, using voltage steps of 0.15 mV and the working electrode is placed on the *trans* side of the interface (this denotes the interior of the droplet not containing proteins).

## RESULTS AND DISCUSSION OF DIB CHARACTERIZATION

### Lipid-only Membranes

EIS and CV measurements (Figure 4(a, b)) are first conducted on DPhPC DIBs that do not contain proteins. Estimates of the near-DC resistance (low-frequency

asymptote),  $R$ , and capacitance,  $C$ , for each DIB are taken from the impedance measurements by fitting an equivalent circuit (a resistor and capacitor in parallel) to the experimental data. Measured membrane resistance values varied from 100 M $\Omega$ –10 G $\Omega$  while capacitance values were typically 200–1000 pF for 300 nL droplets. The area of the bilayer interface is estimated from the capacitance measurements by assuming a specific capacitance of 0.6  $\mu\text{F}/\text{cm}^2$  for DPhPC bilayers (Baba et al., 1999; Funakoshi et al., 2006). CV measurements show the measured current flowing through a lipid bilayer for an increasing and decreasing applied potential from  $-100$  mV and  $+100$  mV. Also shown is the specific resistance (resistance  $\times$  membrane area) and equivalent diameter of the lipid bilayer versus time for successive EIS measurements on three different DIB formation trials (Figure 4(c)). Without proteins in these bilayers, the three trials show that the resistance increases over time (up to 200%), yet the size of the bilayer undergoes a much smaller change (less than 25%). Tracking bilayer size confirms that changes to the nominal resistance are not due solely to changes in bilayer size. The bilayer failure potential using CV is also recorded in order to characterize the electrical limits of DIBs. The current flowing through the membrane is measured for a steadily increasing voltage until rupture, marked by a large spike in the current due to the failure of the membrane resistance. The data shown in Figure 4(d) illustrates that BLMs formed using the DIB technique fail at applied potentials ranging from 100 mV to more than 200 mV lower than values measured for planar bilayer lipid membranes formed using other techniques and more than 1V lower than vesicle bilayers (Needham and Hochmuth, 1989). DPhPC bilayer lipid membranes formed across the pore of a supporting substrate in two separate studies using the folding technique exhibited failure potentials of 390–410 mV (Robello and Gliozzi, 1989; Baba et al., 1999). The bilayer lipid membranes formed in these studies were smaller, however, which

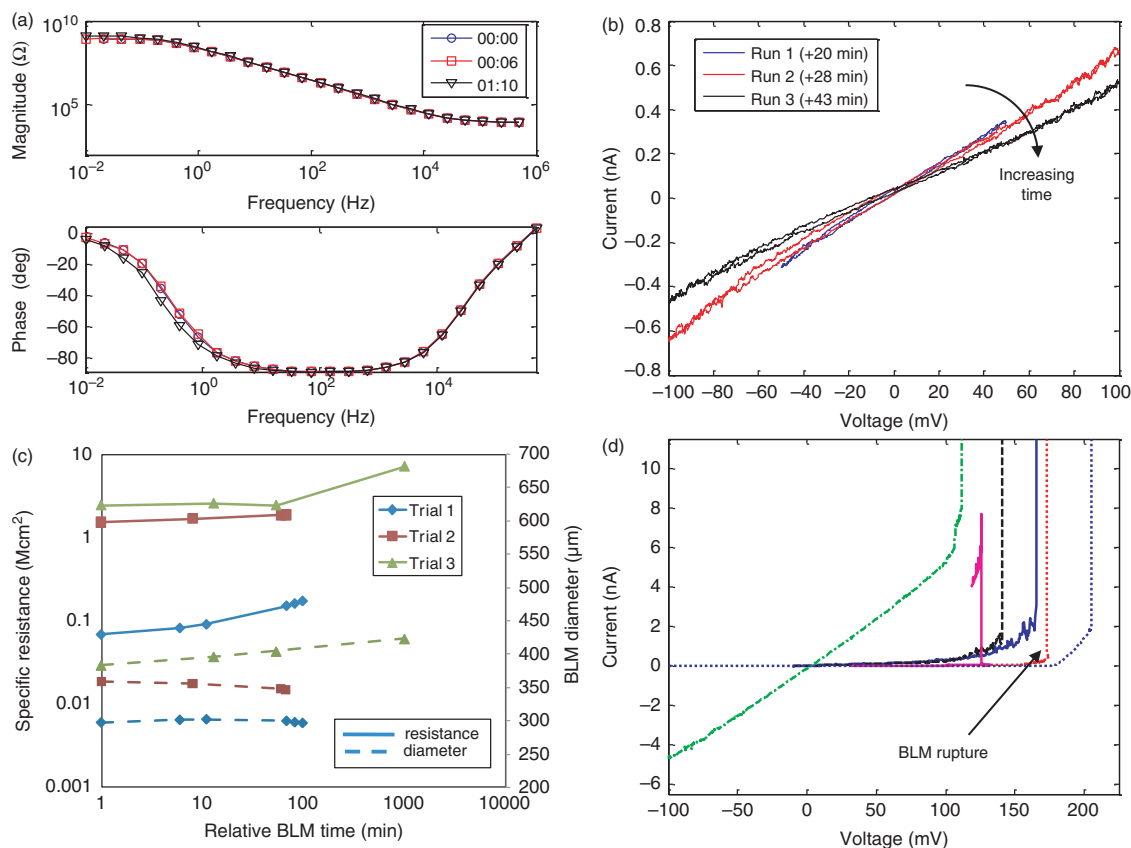


**Figure 4.** The magnitude and phase of the electrical impedance vs frequency for a DIB without proteins measured over time (a). Current vs voltage plotted for three successive CV measurements on a single lipid-only DIB (b). The specific resistance ( $M\Omega\text{cm}^2$ ) and equivalent membrane diameter ( $\mu\text{m}$ ) for three DPhPC DIBs measured in time (c). Failure potentials for DIBs are marked at the point where current increases abruptly (d). Note: The relative time markers indicate the time (in h:min format) after the two droplets first come together to form a bilayer lipid membrane.

may contribute to a more durable lipid membrane (the apertures in the supporting substrate ranged from 100 to 250  $\mu\text{m}$ , resulting in a bilayer with an even smaller diameter when the formation of an annulus of lipid solution around the rim of the pore is considered (Lauger et al., 1967; Wilburn et al., 2006)). In contrast, the diameters of DIBs formed in this study are twice as large. We believe that the combination of a much larger membrane area and a varying degree of monolayer assembly give rise to an increased probability of defect, resulting in lower, more widely spread values of failure potential.

#### ELECTRICAL MODEL OF A DIB

The electrical characterization of bilayer lipid membranes formed using the DIB method confirms the interfacial membrane can be modeled as resistor,  $R$ , and capacitor,  $C$ , in parallel for frequencies up to approximately 10 kHz. The resistance of the aqueous buffer,  $R_e$ , dominates at higher frequencies as shown in the expression for the open-loop electrical impedance:

$$Z_{\text{DIB}}(\omega) = \frac{R}{1 + j\omega RC} + R_e. \quad (1)$$

It should be noted that determining equivalent electrical models for supported or suspended BLMs on substrates

is often more complicated due to the contribution of the substrate (Sundaresan et al., 2008). Using the DIB technique, the resistance of the membrane is dependent on the lipid packing density of each monolayer and the area of the droplet interface, while the capacitance is governed by interfacial area as well as the thickness of the membrane. Voltammetry measurements show that DIBs can withstand potentials as high as 100–220 mV without rupture and have a near-linear current–voltage relationship for potentials less than  $\pm 100$  mV.

#### Lipid Membranes with $\alpha\text{HL}$

$\alpha\text{HL}$  from the bacteria *S. aureus* (Sigma) causes lysis, or cell death, by permeabilizing the cell membrane through the formation of water-permeable ion channels that span the thickness of the membrane (Song et al., 1996). These proteins are dissolved in the aqueous buffer of one droplet (*cis*) in a DIB pair. Three different concentrations of  $\alpha\text{HL}$  are used: 10, 5, and 1  $\mu\text{g}/\text{mL}$  are dissolved in the aqueous buffer solution and kept refrigerated for up to a week. These concentrations are six orders of magnitude higher than those used in studies aimed at discerning single or few-protein insertion events (Wong, Jeon and Schmidt, 2006;

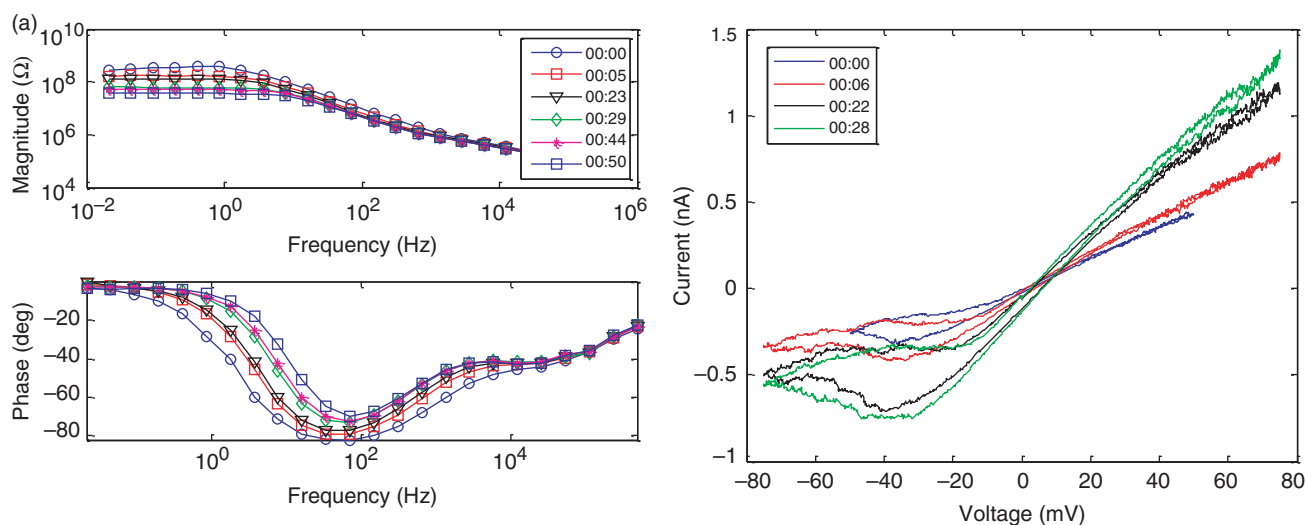
Holden, Needham and Bayley, 2007; Hwang et al., 2007) because it is desired to cause and record large-scale changes to the lipid membranes.

Figure 5 illustrates the measured effects of  $5\ \mu\text{g}/\text{mL}$   $\alpha\text{HL}$  in buffer solution added to one droplet in the droplet pair. Successive EIS measurements show a reduction in the resistance of the lipid membrane (Figure 5(a)). Furthermore, CV measurements indicate that the incorporation of the ion channels into the membrane alters the current–voltage relationship compared to bilayers, which do not incorporate  $\alpha\text{HL}$ . Comparing Figure 4(b) and Figure 5(b) we see that the incorporation of the  $\alpha\text{HL}$  into the interfacial bilayer produces a non-linear current–voltage relationship that exhibits an inflection point in the current at voltages less than approximately  $-20\ \text{mV}$ . The CV data also indicates that the conductance (as measured by the slope of the current–voltage curve) of the lipid membrane containing ion channels increases over time as additional  $\alpha\text{HL}$  incorporate into and porate the membrane. This response is consistent with the impedance spectroscopy results.

The insertion and activity of  $\alpha\text{HL}$  ion channels in DIBs is witnessed as both a continual reduction in the resistance of the bilayer as well as a non-linear current–voltage relationship measured with CV. Song et al. (1996) characterized the structure and function of the 33 kDa  $\alpha\text{HL}$  ion channel from the *S. aureus* bacteria and provided evidence that a water-pore forms when seven  $\alpha\text{HL}$  monomers aggregate on the lipid surface to form a heptamer. The heptamer then inserts through the lipid bilayer, creating an anion-selective water channel. The data shown in Figure 5, and in Figure 6 for three different concentrations of ion channels, indicate that the insertion of a large number of  $\alpha\text{HL}$  heptamers reduces the effective resistance of a lipid bilayer. Measured initial specific resistances of droplet–interface bilayers ranged from 0.01

to  $10\ \text{M}\Omega\text{cm}^2$  (Figure 6(a)), and these values then decreased by more than an order of magnitude in the first 1–2 h after BLM formation. The final resistance values measured for the  $\alpha\text{HL}$ -permeabilized lipid membranes ranged from 1 to  $100\ \text{M}\Omega$ . During our experiments, rarely did the membranes rupture during the 1- to 2-h time period of monitoring. However, it is envisioned that at some point the bilayer would become saturated with functioning ion channels and its resistance would either reach a minimum value or the membrane would fail causing the droplets to coalesce. The fate of the membrane would thus be determined by the supplied concentration of the  $\alpha\text{HL}$  channels within the droplet. This process in nature is called lysis, or cell death by breaking of the membrane (Song et al., 1996); hence the name ‘hemolysin,’ which means lysis of the red blood cells (Figures 4(c) and 6(b)). In contrast, the measured values of resistance for lipid membranes without ion channels increased over time as phospholipids from the surrounding bulk lipid solution re-assemble at the oil/water interface after manual electrode insertion and droplet manipulation (a process which damages the lipid assemblies).

$\alpha\text{HL}$  ion channels residing in the interface bilayers display non-linear current–voltage response during CV measurements. Partial rectification of the ion current is seen at negative applied *trans* potentials (which correspond to positive *cis* potentials) below roughly  $-40\ \text{mV}$  in Figure 5(b). Others have witnessed similar asymmetric rectification of the ionic current through  $\alpha\text{HL}$  ion channels reconstituted in bilayer lipid membranes at positive *cis* potentials and have attributed this behavior to an asymmetric charge distribution of the amino acid residues along the transmembrane pore (Henrickson et al., 2000; Aksimentiev and Schulten, 2005; Merzlyak et al., 2005). Furthermore, Menestrina characterized



**Figure 5.** EIS (a) and CV (b) measurements for a single DIB in which one droplet contained  $5\ \mu\text{g}/\text{mL}$   $\alpha\text{HL}$  dissolved in buffer solution. The working electrode was placed in the droplet without protein (*trans*).

the voltage-dependent conductance of  $\alpha$ HL ion channels, finding that the ion channel is inhibited by divalent and trivalent cations (Menestrina, 1986). In these studies, however, no inhibition was seen for the monovalent sodium cations dissolved in the buffer solution. It should also be noted that the non-linear current–voltage relationships shown in Figure 5(b) were measured for lipid bilayers containing many  $\alpha$ HL ion channels and these data may reflect both the occurrence of current rectification through ion channels residing in the membrane as well as the continued insertion of additional channels into the bilayer (which leads to the increased conductance observed in subsequent CV measurements).

### Lipid Membranes with Alamethicin

The results demonstrated with  $\alpha$ HL provide credible evidence that the insertion of proteins into a lipid bilayer produces variations in the current–voltage relationship of the membrane. To further illustrate that this altered response is protein dependent, a second series of tests are performed using the protein alamethicin. Purified alamethicin from the fungus *T. viride* (Sigma and A.G. Scientific) is reconstituted into bilayer lipid membranes in a similar manner. The alamethicin is stored in ethanol at 0.1% (w/v) and this stock solution is diluted further to a concentration of 1  $\mu$ g/mL alamethicin in aqueous buffer. Alamethicin is a 2 kDa ion channel that binds to and partially inserts into a bilayer as a monomer and then upon application of voltage, inserts through the hydrophobic core of the membrane (Archer and Cafiso, 1991; Bechinger, 1997). The instability of the

hydrophilic amino acids in the peptide chain then drives aggregation ( $3 < n < 12$  per bundle) with other monomers to form a cation-selective, voltage-dependent ion channel (Archer and Cafiso, 1991; He et al., 1996). The EIS and CV measurements on bilayers containing alamethicin confirm this behavior (Figure 7).

The observed non-linear current–voltage behavior (Figure 7(a)) agrees well with measurements of alamethicin in supported bilayer lipid membranes (Vodyanoy et al., 1983, 1988; Archer and Cafiso, 1991; Romer and Steinem, 2004; Wong et al., 2006). Protein activation (opening) consistently occurred at potentials (relative to the *cis* side of the membrane) between  $-25$  mV and  $-80$  mV for the concentrations used in these tests. Often successive CV measurements on the same bilayer with alamethicin showed little change over time (Figure 4), indicating that a large percentage of the proteins that incorporated into the BLM did so before the first CV measurement (performed within 10–20 min after BLM formation). This behavior is expected, since alamethicin monomers are known to bind to and partially insert into a bilayer prior to the application of a voltage (Archer and Cafiso, 1991; Bechinger, 1997). The measured data support this behavior, suggesting that the alamethicin monomers attach to the lipid monolayer prior to BLM formation, and therefore, are ready to insert upon the first voltammetry measurement. Hysteresis in the CV measurements was seen in some trials and is linked to both the opening/closing rates of the ion channels as well as the applied voltage ramp rate (Vodyanoy et al., 1988; Okazaki et al., 2003). Vodyanoy et al. (1983) also performed studies that indicate adsorbed alamethicin monomers can alter the geometric capacitance of a

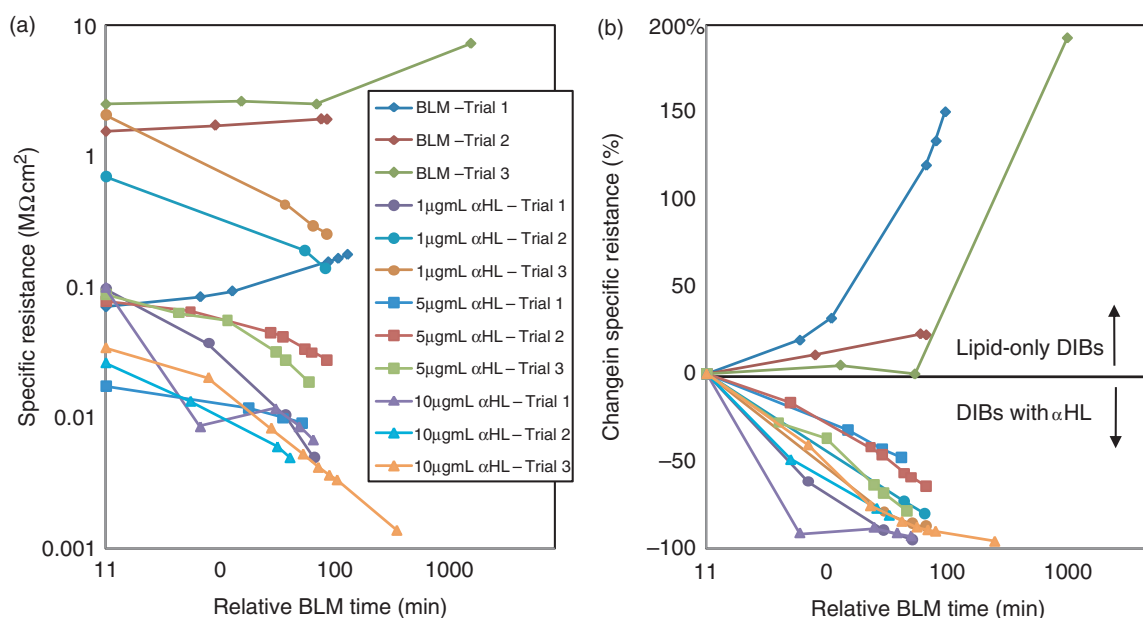


**Figure 6.** Specific resistance ( $M\Omega \cdot cm^2$ ) (a) and change in specific resistance (%) (b) vs time after BLM formation for DIBs containing varying amounts of  $\alpha$ HL (1, 5, and 10  $\mu$ g/mL).

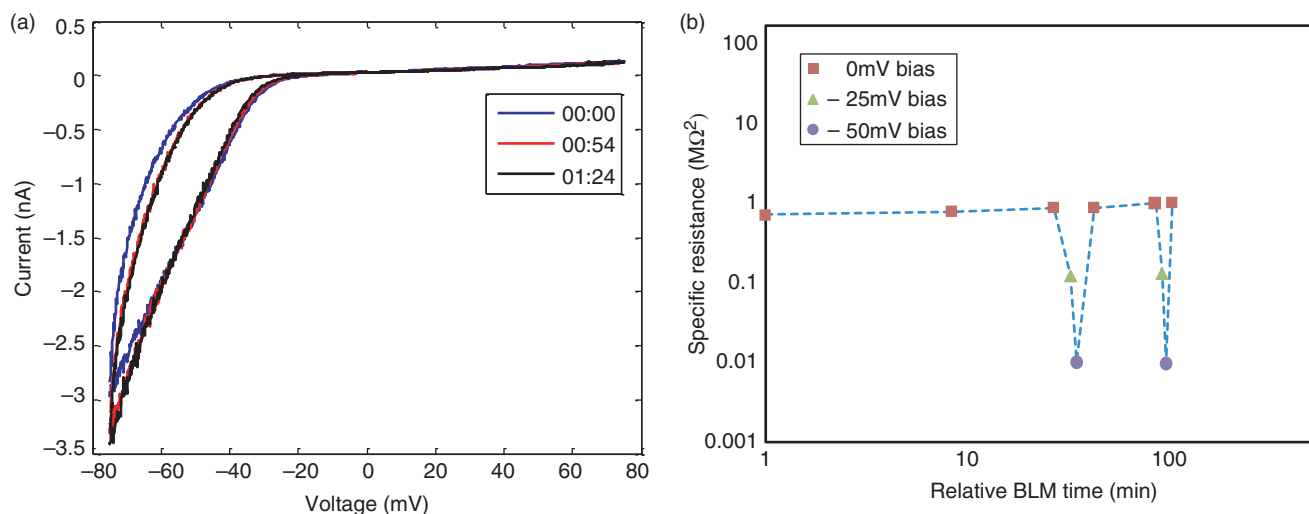


**Figure 7.** The current–voltage relationship (a) and the specific bilayer resistance vs time (b) measured for an interface bilayer with  $1 \mu\text{g/mL}$  alamethicin added to one droplet. EIS measurements were performed at three different biasing potentials (0,  $-25$ , and  $-50$  mV) and demonstrate the ability to toggle the resistance of the bilayer with an applied bias potential.

bilayer and that the charging and discharging of the total capacitance is affected by the corresponding rates of alamethicin adsorption and desorption from the membrane.

The working electrode in these tests is placed in the droplet containing only buffer solution (*trans*), therefore an applied potential more negative than  $-50$  mV is required to open all alamethicin channels. Bilayers containing alamethicin produced small non-zero ( $<5$  mV) open-circuit potentials, further indicating that the applied voltage causes pore opening in the alamethicin channels and that in the open-circuit configuration, the ion channels are in a closed state. The specific membrane resistance is reversibly varied from  $1 M\Omega \text{cm}^2$  at  $0$  mV in the closed state to  $0.1 M\Omega \text{cm}^2$  at  $-25$  mV in a partially open state and to  $0.01 M\Omega \text{cm}^2$  at  $-50$  mV in a fully open state (Figure 7(b)). The bilayer is returned to its open-circuit state between EIS measurements, verifying that the reduction in the specific resistance at  $-50$  mV was not dependent on a previous measurement  $-25$  mV. Furthermore, the resistance of the bilayer in the closed state remained steady, and in some trials increased slightly, over the duration of the test as excess lipid molecules in the surrounding lipid solution re-assemble at the oil/water interface following droplet manipulation. Multiple DIB pairs ( $n=9$ ) containing alamethicin in one droplet further support the current–voltage relationship of alamethicin in a bilayer shown in Figure 7. In all tests, the conductance of the membrane increased 2–3 orders of magnitude by alamethicin activation.

## FEEDBACK CONTROL OF DIB

Feedback control offers an additional, previously unexplored route for tailoring ion transport across

bilayer lipid membranes and provides methods to obtain a controllable droplet network for use as nano-reactors or bio-communication devices. In this work, integral current control and proportional–integral (PI) voltage control are demonstrated on a two-droplet pair adjoined by a single bilayer interface.

A detailed discussion of the experimental setup for performing feedback control of DIBs is provided in the Appendix. The control analysis used in the selection and design of each compensator is also included for clarity.

## Feedback Current Control through a Lipid Bilayer

Feedback current tracking in order to prescribe a desired current flowing through a lipid bilayer is demonstrated on a DIB without proteins. First, the electrical impedance of the lipid bilayer is measured in order to obtain estimates of the bilayer resistance and capacitance. These values provide a way to simulate the closed-loop system admittance and iteratively select an appropriate integral gain value in order to achieve current matching.

Feedback current control of ions flowing through a DIB was applied via the same electrodes inserted into the droplets for positioning and electrical measurements. The integral compensator (shown in Figure 8) used in this scheme computes a corrective control voltage applied to drive the error between the measured current and the desired value toward zero. A  $100$  pA sinusoidal waveform is selected for the amplitude of the desired current signal in this demonstration. The ability to track this waveform is measured experimentally at four driving frequencies,  $f_d$ , using a constant integral control gain.

The experimental measurements in Figure 9 confirm the simulated closed-loop dynamics that as the driving frequency increases above  $10$  mHz, the actual current flowing through the bilayer does not track the desired

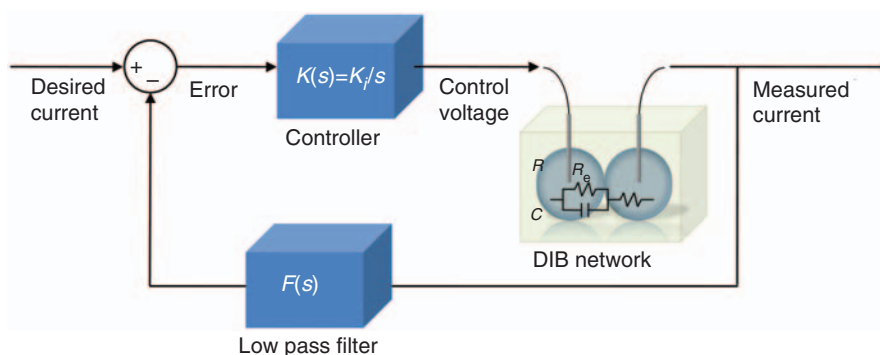


**Figure 8.** Block diagram of feedback current control applied to a DIB.

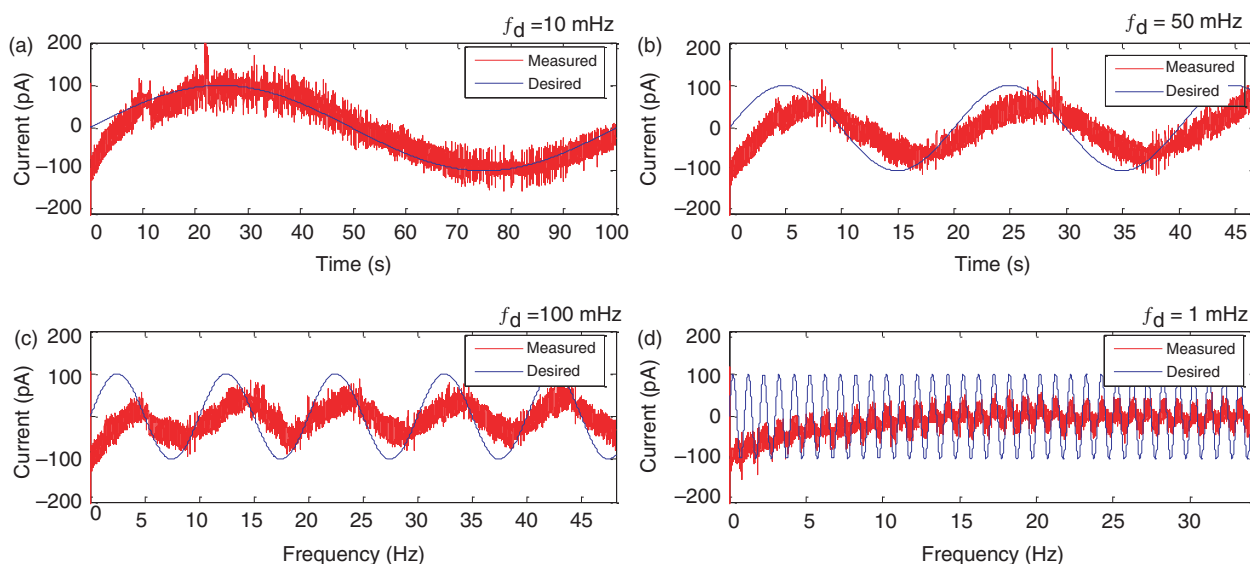


**Figure 9.** Measured current tracking vs driving frequency,  $f_d$ , of a DIB without proteins (a–d).

current waveform accurately. The measured current for a driving frequency of 50 mHz has a slightly smaller amplitude and lags the desired current by 2–3 s in time. At 100 mHz, the amplitude of the measured signal is roughly half of the 100 pA desired amplitude and a similar phase lag exists. Lastly, the measurement at 1 Hz shows significant attenuation of the measured current, even though it is able to keep pace in time with the desired current.

The performance of the current tracking routine is limited to low frequency tracking (up to  $\sim 10$  mHz) but demonstrates the ability to prescribe desired current flow across a bilayer membrane. Increasing the control gain is one way to achieve better tracking at higher driving frequencies, though at the expense of a larger control voltage (this trade-off must be considered as the membrane can fail at potentials near 200 mV). Eliminating the external low-pass filter from the feedback loop would also increase the operational bandwidth but requires being able to measure current within a lower current range in Autolab in order to increase the magnitude of the voltage proportional to the measured current. This analysis provides evidence that biological

systems and their dynamics can be tailored in ways other than by component selection. Feedback current control provides an alternative method to regulate ion flux across a lipid membrane and in a system consisting of multiple connected droplets, closed-loop current control may provide a way to carry out precise chemical reactions, including various enzymatic reactions (Vriezema et al., 2007), within specific droplets at desired rates.

### Feedback Voltage Control for Tunable Resonance

A second closed-loop control strategy is employed to investigate the ability to create a tunable resonance of the voltage across a bilayer lipid membrane. Specifically, PI voltage feedback control transforms the first-order impedance response of the bilayer lipid membrane into a second-order closed-loop response, characterized by a resonance peak whose properties depend on both the electrical behavior of the lipid membrane and the applied control gains. The proportional and integral gains used in feedback voltage control are computed from measured values of electrical resistance,  $R$ , and capacitance,  $C$ , of a lipid bilayer obtained from

impedance spectroscopy and the prescribed values of natural frequency,  $f_n$  (or  $\omega_n$  in rad/s), and damping,  $\zeta$ , for the closed-loop system. Expressions for these gains derived from the open-loop electrical impedance (see Appendix for complete analysis) of the bilayer lipid membrane are given by:

$$K_P = \frac{\omega_n RC(2B\zeta - A\omega_n) - B}{A^2\omega_n^2 - 2\zeta\omega_n AB + B^2}, \quad (2)$$

and

$$K_I = \frac{\omega_n^2(RCB - A)}{A^2\omega_n^2 - 2\zeta\omega_n AB + B^2}, \quad (3)$$

where  $A = R_e \cdot R \cdot C$ ,  $B = R + R_e$ , and recall that  $R_e$  is the resistance of the electrolyte solution within the droplets. The closed-loop transfer function of the voltage across the membrane relative to the desired voltage is measured during feedback voltage control on several DIBs with and without proteins. A 50 mV (RMS) white noise waveform is used as the input for measuring closed-loop transfer functions.

#### VOLTAGE CONTROL OF LIPID-ONLY DIBS

The closed-loop transfer function of a DPhPC DIB without proteins is transformed from the first-order, open-loop electrical impedance response (Figure 4(a)) to a second-order closed-loop system using PI feedback voltage control (Figure 10(a)). In each trial, the electrical resistance and capacitance of the membrane are approximated from impedance measurements. The proportional and integral control gains,  $K_P$  and  $K_I$ , are then computed in order to produce a closed-loop system with a desired natural frequency and damping ratio.

Figure 10(a) shows successive measurements of the frequency response function (FRF) for a bilayer where

the natural frequency and damping ratio were chosen as 1 Hz and 0.1, respectively. The measured FRFs of the bilayer in closed-loop control match the simulated response fairly well in the location of the resonance peak, but the measured result has more damping than expected from the simulation as indicated by the reduced magnitude of the FRF near resonance. These differences are attributed to inaccurate estimates of the membrane resistance and capacitance from EIS data but also due to non-linear decreases in the resistance and increases in the capacitance (Alvarez and Latorre, 1978) of the bilayer with respect to a larger potential developed across the membrane at resonance. The magnitude of the measured resonance peak increases over time, which is attributed to the increased resistance of the BLM due to continued re-assembly of phospholipids into the membrane (as seen in the EIS and CV data of lipid-only DIBs in Figure 4).

Additional trials show that the natural frequency of the closed-loop system can be set at frequencies higher than 1 Hz. Figure 10(b) presents the frequency response functions of a single DIB in which the proportional and integral gains are adjusted to set the closed-loop natural frequency at 1, 10, and 100 Hz in separate trials. The measurements of the closed-loop system confirm that through feedback control the dynamics of a changing voltage across the bilayer can be operated at much higher frequencies than in the open loop, defined by the electrical impedance of the membrane. The impedance spectra plotted in Figures 4(a) and 5(a) show that the bandwidth of the electrical impedance ranges from 0.1–10 Hz, but at higher frequencies the magnitude of the impedance drops off and the phase delay increases. This open-loop response indicates that a voltage developed across a lipid bilayer as the result of current flowing through it, attenuates at frequencies higher than 1 Hz. Through feedback control, however, the voltage

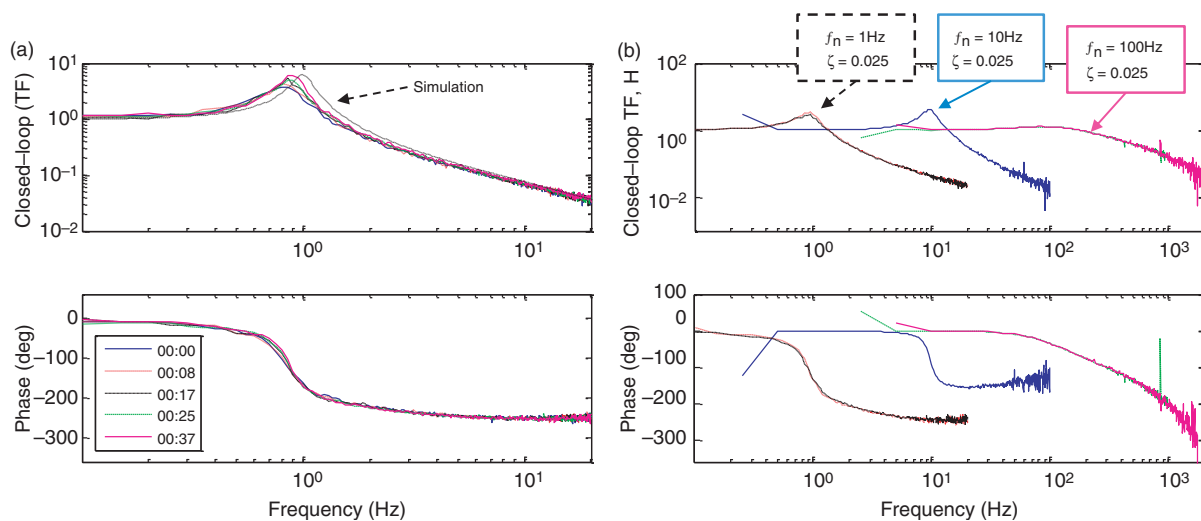


**Figure 10.** Measured closed-loop frequency response functions of a DIB without proteins for a natural frequency at 1 Hz and a damping ratio of 0.1 (a). Measured closed-loop FRFs on a single DIB demonstrate the ability to place the resonance and that the bandwidth of operation can be increased from less than 1 Hz to more than 100 Hz.

across the bilayer can be operated at frequencies within the lower end of the audible range (20–20,000 Hz). The measurements also show that at natural frequencies of 100 Hz and higher, the bilayer exhibits significantly higher damping evident by the diminished peak height. This behavior may indicate a possible frequency dependence of the electrical resistance and capacitance of the bilayer. Physically, the operation bandwidth is limited by amount of increasing level of current required to develop a potential across the bilayer at higher frequencies, which could cause bilayer failure. Several feedback control trials in which the natural frequency was placed at 200 Hz or higher caused the droplets to coalesce when the bilayer ruptured.

### VOLTAGE CONTROL OF LIPID BILAYERS WITH ALAMETHICIN

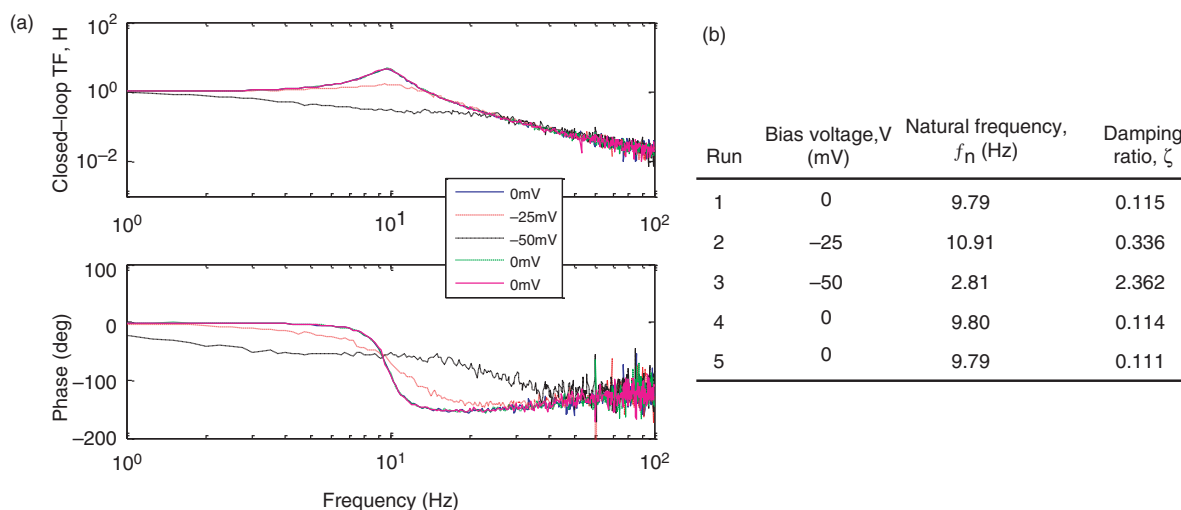
Coupling the voltage-dependent behavior of a bilayer containing alamethicin proteins and feedback voltage control provides a way of reversibly controlling the magnitude of the resonance peak. In a bio-communications application, the use of a bias potential to regulate the resistance of the membrane by triggering the proteins changes the amplification of the voltage across the membrane. The same feedback control scheme was applied to DIBs in which one of the two droplets contained alamethicin.

Figure 11(a) shows the measured frequency response functions of a single bilayer containing alamethicin (EIS and CV data for this same DIB are shown in Figure 7). A natural frequency of 1 Hz and a damping ratio of 0.025 are selected and the control gains are computed using resistance and capacitance values (775 M $\Omega$  and 750 pF, respectively) measured at 0 mV bias. A bias voltage is added to the white noise input during the measurement at different potentials in order to vary the membrane resistance between 800 and 8 M $\Omega$  as

discussed earlier in this article. The change in the membrane resistance inversely affects the damping ratio of the closed-loop system and results in a significant change in the magnitude of the resonance peak in the frequency response function. With 0 mV bias and the alamethicin channels closed, the high resistance of the membrane results in lower damping and a higher resonance peak. Partial protein activation by the resonance voltage may explain the additional damping (0.11 vs. 0.025) in the measurements taken at 0 mV bias. Conversely, the height of the resonance peak is reduced partially with a 25 mV bias (some alamethicin channels open) and then nearly eliminated at –50 mV (all alamethicin channels open). Estimates of natural frequency and damping ratio confirm that the damping ratio increases at the negative bias potentials when the alamethicin ion channels are opened Figure 1(b). These measurements demonstrate that coupling external feedback control with the voltage-gating characteristics of alamethicin provides a way to reversibly control the amplification of the voltage across the bilayer.

### CONCLUSIONS

The DIB technique enables the formation of complex biomolecular networks that have controllable ion transport properties. This technique, which relies on the self-assembly of lipid molecules to form monolayers at an oil/water interface, creates bilayer lipid membranes at the interfaces of adjoined water droplets. The contents of the droplets can be tailored in order to study protein and ion channel activity at the interface.  $\alpha$ HL ion channels, which create water-permeable pathways through the lipid membrane, cause degradation of the membrane as measured by the electrical resistance of the BLM. Alamethicin ion channels offer additional



**Figure 11.** Measured FRFs of a bilayer with alamethicin proteins at different bias potentials (a). Estimates of the natural frequency and damping ratio by fitting the measured frequency responses (using *INVREQS* in *Matlab*) confirm that toggling the bias voltage alters the membrane resistance, which primarily affects the damping ratio of the system.

control of the permeation of lipid bilayers, due to their voltage-dependent opening and closing. These findings verify that the selection and incorporation of proteins provide a convenient way to obtain highly diverse active lipid membranes that employ the inherent functionality of the biomolecules.

Feedback control of ion transport across biological molecules is a novel method for prescribing complex, rate-specific, and multi-directional processes in a large network. Two different feedback control schemes are demonstrated in this article on DIB: integral feedback current tracking and PI feedback voltage control. The ability to combine control techniques and biological materials provides a starting point for creating controlled biosystems by tailoring interfaces to have prescribed current–voltage relationships. The applications that could evolve from these types of studies range from controlled nanoreactors for conducting small-scale chemical and biochemical reactions to complex DIB networks for conducting a diverse arrays of protein studies involving chemical, optical, and mechanical stimuli.

## ACKNOWLEDGEMENTS

The authors would like to acknowledge financial support through Office of Naval Research (N000140810654) as well as supplemental funding from the Virginia Space Grant Consortium (VSGC). Thanks also to Dr David Needham of Duke University for engaging discussions on the formation of droplet-interface bilayers.

## APPENDIX

### Feedback Control System Setup

Feedback control of DIBs requires the ability to continually compare a measured quantity (current or voltage) with a desired signal. The Autolab PGSTAT12, controlled externally, is used to produce and measure current and voltage during the study (Figure A1). The feedback control algorithms for both integral current control and PI voltage control are computed in Simulink, and the appropriate control signals, in the form of voltages, are output to Autolab via a dSPACE CP1104, 4-channel control board. Autolab accepts the control signal and produces the appropriate voltage or current applied to the electrodes inserted into the droplets. The Autolab system is configured to also output voltage signals back to dSPACE that are proportional to the current flowing through the bilayer and the voltage across it in order to complete the feedback loop. It should be noted that during feedback

current control, Autolab is operated in potentiostatic mode, regulating the voltage across the membrane. During the feedback voltage control tests, Autolab is operated in galvanostatic mode, such that it regulates the current flowing through the bilayer, and a Tektronix 2630 Fourier Analyzer is used to compute the frequency response functions of the closed-loop system. A 50 mV (RMS) random white noise voltage is generated by Tektronix and added to the bias potential created in Simulink for exciting the bilayer systems. Closed-loop transfer functions are recorded with 5 kHz sampling rate in dSpace and consist of 10 averages of 1024 frequency points within the tested range. Also, an Ithaco 4302 low pass filter (4-pole Butterworth filter) with a cutoff frequency at 50 Hz is used to filter noise from the voltage signal proportional to the measured current only during feedback current control.

### Compensator Design for Integral Current Control

The goal in feedback current control is to minimize the error between a desired current signal and the current flowing through the membrane (Figure 9). The transfer function of the integral controller is:

$$K(s) = \frac{K_I}{s}, \quad (1)$$

where  $K_I$  is the integral gain used to increase or decrease the control authority and  $s$  is the Laplace variable. Since the input to the system is an applied voltage and the output is a current flowing through the bilayer, the plant is described by the electrical admittance,  $Y(s)$ , of the system. The electrical impedance,  $Z(s)$ , of two-droplet network written in the  $s$ -domain, which is modeled as a resistor,  $R$ , and capacitor,  $C$ , connected in parallel for the bilayer in series with a resistance,  $R_e$ , for the aqueous solution, is given by:

$$Z(s) = [R||C] + R_e = \frac{R}{1 + sRC} + R_e. \quad (2)$$

Simplifying the expression for electrical impedance, gives:

$$Z(s) = \frac{As + B}{1 + sRC}, \quad (3)$$

where  $A = R_e \cdot R \cdot C$ ,  $B = R + R_e$ , and  $Z(s) = 1/Y(s)$ . Therefore, the admittance of the system can be written as:

$$Y(s) = \frac{1 + sRC}{As + B}. \quad (4)$$

The transfer function for the 4-pole, low-pass Butterworth filter with a cutoff frequency at 50 Hz is:

$$F(s) = \frac{\alpha_0}{s^4 + \alpha_3 s^3 + \alpha_2 s^2 + \alpha_1 s + \alpha_0}, \quad (5)$$

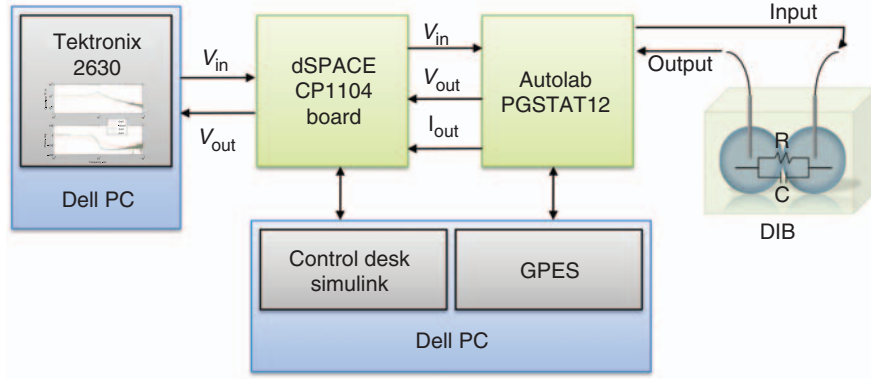


**Figure A1.** Schematic of the equipment and software used for feedback control of DIBs. The Tektronix 2630 was used for measuring frequency response functions of the bilayers only during closed-loop voltage control.

where the coefficients that were determined experimentally are  $\alpha_0 = 9.741 \times 10^9$ ,  $\alpha_1 = 8.102 \times 10^7$ ,  $\alpha_2 = 3.370 \times 10^5$ , and  $\alpha_3 = 820.9$ .

The closed-loop transfer function for integral control,  $H_I(s)$ , is:

$$H_I(s) = \frac{K(s)Y(s)}{1 + F(s)K(s)Y(s)} = \frac{K_I(1 + sRC)}{As^2 + Bs + F(s)K_I(1 + sRC)}. \quad (6)$$

The selection of the  $K_I$  gain determines how much control effort is afforded in order to drive the actual current toward the desired current. Simulated closed-loop responses were generated using Equation (6) and compared with current measurements performed at five frequency points.

#### Compensator Design for PI Voltage Control

Feedback voltage control of DIBs demonstrates that the natural dynamics of lipid membranes can be modified to provide desired closed-loop dynamics such as damping ratio and natural frequency using pole-placement. The plant in this case is the electrical impedance,  $Z(s)$ , given in Equations (2) and (3). PI control applied to the impedance of the bilayer, creates a second-order closed-loop system, which can be characterized by a natural frequency,  $\omega_n$ , and damping ratio,  $\zeta$ . The transfer function of a PI controller is defined as:

$$K_{PI}(s) = K_P + \frac{K_I}{s}, \quad (7)$$

where  $K_P$  is the proportional gain and  $K_I$  is again the integral gain. Since the plant is defined by the electrical impedance of the bilayer system, the closed-loop transfer function,  $H_{PI}$ , can be written as:

$$H_{PI}(s) = \frac{K_{PI}(s)Z(s)}{1 + K_{PI}(s)Z(s)} \quad (8)$$

and then expanded, using the relations in Equations (3) and (7), to:

$$H_{PI}(s) = \frac{AK_P s^2 + (AK_I + BK_P)s + BK_I}{(RC + AK_P)s^2 + (AK_I + BK_P + 1)s + BK_I}. \quad (9)$$

The characteristic equation that defines the closed-loop dynamics of the system is:

$$s^2 + \left(\frac{AK_I + BK_P + 1}{RC + AK_P}\right)s + \left(\frac{BK_I}{RC + AK_P}\right) = 0, \quad (10)$$

where,

$$2\zeta\omega_n = \left(\frac{AK_I + BK_P + 1}{RC + AK_P}\right), \quad (11)$$

$$\omega_n^2 = \left(\frac{BK_I}{RC + AK_P}\right). \quad (12)$$

Equations (11) and (12) relate the electrical parameters of the DIB network as well as the two gains for the controller,  $K_{PI}(s)$ , to the natural frequency and damping ratio of the closed-loop system. These expressions can also be written in matrix form:

$$\begin{bmatrix} \omega_n^2 A & -B \\ 2\zeta\omega_n A - B & -A \end{bmatrix} \begin{bmatrix} K_P \\ K_I \end{bmatrix} = \begin{bmatrix} -\omega_n^2 RC \\ 1 - 2\zeta\omega_n RC \end{bmatrix}, \quad (13)$$

where the control gains can be computed for measured electrical properties of the DIB network and for desired closed-loop natural frequency,  $\omega_n$ , and damping ratio,  $\zeta$ . Analytical expressions for the two control gains are given by:

$$K_P = \frac{\omega_n RC(2B\zeta - A\omega_n) - B}{A^2\omega_n^2 - 2\zeta\omega_n AB + B^2} \quad (14)$$

and

$$K_I = \frac{\omega_n^2(RCB - A)}{A^2\omega_n^2 - 2\zeta\omega_n AB + B^2}. \quad (15)$$

Equations (14) and (15) illustrate that feedback control can provide a way to tailor the closed-loop electrical impedance of DIBs. The connection between the closed-loop dynamics and the electrical properties of the membrane for fixed control gains makes it possible to detect changes to the resistance and capacitance of the membrane due to lipid packing and/or ion channel insertion. Values for  $K_P$  and  $K_I$  are computed for each bilayer system and for prescribed values of damping ratio and natural frequency.

## REFERENCES

- Aksimentiev, A. and Schulten, K. 2005. "Imaging {alpha}-Hemolysin with Molecular Dynamics: Ionic Conductance, Osmotic Permeability, and the Electrostatic Potential Map," *Biophysics Journal*, 88(6):3745–3761.
- Alvarez, O. and Latorre, R. 1978. "Voltage-dependent Capacitance in Lipid Bilayers Made from Monolayers," *Biophysics Journal*, 21(1):1–17.
- Andersen, O.S. 1983. "Ion Movement through Gramicidin A Channels. Single-channel Measurements at Very High Potentials," *Biophysics Journal*, 41(2):119–133.
- Archer, S.J. and Cafiso, D.S. 1991. "Voltage-dependent Conductance for Alamethicin in Phospholipid Vesicles. A Test for the Mechanism of Gating," *Biophysics Journal*, 60(2):380–388.
- Baba, T., Toshima, Y., Minamikawa, H., Hato, M., Suzuki, K. and Kamo, N. 1999. "Formation and Characterization of Planar Lipid Bilayer Membranes from Synthetic Phytanyl-Chained Glycolipids," *Biochimica et Biophysica Acta (BBA) – Biomembranes*, 1421(1):91–102.
- Bechinger, B. 1997. "Structure and Functions of Channel-forming Peptides: Magainins, Cecropins, Melittin and Alamethicin," *Journal of Membrane Biology*, 156(3):197–211.
- Bernards, D.A., Malliaras, G.G., Toombes, G.E.S. and Gruner, S.M. 2006. "Gating of an Organic Transistor through a Bilayer Lipid Membrane with Ion Channels," *Applied Physics Letters*, 89(5):053505.
- Castellana, E.T. and Cremer, P.S. 2006. "Solid Supported Lipid Bilayers: From Biophysical Studies to Sensor Design," *Surface Science Reports*, 61:429–444.
- Cheng, Y., Bushby, R.J., Evans, S.D., Knowles, P.F., Miles, R.E. and Ogier, S.D. 2001. "Single Ion Channel Sensitivity in Suspended Bilayers on Micromachined Supports," *Langmuir*, 17(4):1240–1242.
- de Angeli, A., Thomine, S., Frachisse, J.-M., Ephritikhine, G., Gambale, F. and Barbier-Brygoo, H. 2007. "Anion Channels and Transporters in Plant Cell Membranes," *FEBS Letters*, 581(12):2367–2374.
- Duncan, A.J., Leo, D.J. and Long, T.E. 2008. "Beyond Nafion: Charged Macromolecules Tailored for Performance as Ionic Polymer Transducers," *Macromolecules*.
- Evans, D.E., Briars, S.-A. and Williams, L.E. 1991. "Active Calcium Transport by Plant Cell Membranes," *Journal of Experimental Botany*, 42(3):285–303.
- Funakoshi, K., Suzuki, H. and Takeuchi, S. 2006. "Lipid Bilayer Formation by Contacting Monolayers in a Microfluidic Device for Membrane Protein Analysis," *Anal. Chem.*, 78(24):8169–8174.
- Gruen, D.W. and Haydon, D.A. 1981. "A Mean-Field Model of the Alkane-Saturated Lipid Bilayer Above its Phase Transition. II. Results and Comparison with Experiment," 33(2):167–187.
- Hanai, T., Haydon, D.A. and Taylor, J. 1964. "An Investigation by Electrical Methods of Lecithin-in-Hydrocarbon Films in Aqueous Solutions," In: *Proceedings of the Royal Society of London. Series A, Mathematical and Physical Sciences*, (1934–1990), 281(1386):377–391.
- Hanai, T., Haydon, D.A. and Taylor, J. 1965. "Some Further Experiments on Bimolecular Lipid Membranes," *Journal of General Physiology*, 48(5):59–63.
- Haydon, D.A. and Taylor, J. 1963. "The Stability and Properties of Bimolecular Lipid Leaflets in Aqueous Solutions," *Journal of Theoretical Biology*, 4(3):281–296.
- He, K., Ludtke, S.J., Heller, W.T. and Huang, H.W. 1996. "Mechanism of Alamethicin Insertion into Lipid Bilayers," *Biophysics Journal*, 71(5):2669–2679.
- Henrickson, S.E., Misakian, M., Robertson, B. and Kasianowicz, J.J. 2000. "Driven DNA Transport into an Asymmetric Nanometer-scale Pore," *Physical Review Letters*, 85(14):3057.
- Hess, H. and Vogel, V. 2001. "Molecular Shuttles Based on Motor Proteins: Active Transport in Synthetic Environments," *Reviews in Molecular Biotechnology*, 82(1):67–85.
- Hladky, S.B. and Haydon, D.A. 1970. "Discreteness of Conductance Change in Bimolecular Lipid Membranes in the Presence of Certain Antibiotics," *Nature*, 225(5231):451–453.
- Hladky, S.B. and Haydon, D.A. 1972. "Ion Transfer Across Lipid Membranes in the Presence of Gramicidin A: I. Studies of the Unit Conductance Channel," *Biochimica et Biophysica Acta (BBA) – Biomembranes*, 274(2):294–312.
- Holden, M.A., Needham, D. and Bayley, H. 2007. "Functional Bionetworks from Nanoliter Water Droplets," *Journal of American Chemical Society*, 129(27):8650–8655.
- Hwang, W.L., Holden, M.A., White, S. and Bayley, H. 2007. "Electrical Behavior of Droplet Interface Bilayer Networks: Experimental Analysis and Modeling," *Journal of American Chemical Society*, 129(38):11854–11864.
- Lanyi, J.K. and Pohorille, A. 2001. "Proton Pumps: Mechanism of Action and Applications," *Trends in Biotechnology*, 19(4):140–144.
- Lauger, P., Lesslauer, W., Marti, E. and Richter, J. 1967. "Electrical Properties of Bimolecular Phospholipid Membranes," *Biochimica et Biophysica Acta*, 135:20–32.
- Lee, S., Kim, D.H. and Needham, D. 2001. "Equilibrium and Dynamic Interfacial Tension Measurements at Microscopic Interfaces Using a Micropipet Technique. 2. Dynamics of Phospholipid Monolayer Formation and Equilibrium Tensions at the Water-Air Interface," *Langmuir*, 17(18):5544–5550.
- Lewis, K.L., Lianying, S., Hawkrigde, F.M., Ward, K.R. and Rhoten, M.C. 2006. "Immobilization of Cytochrome c Oxidase into Electrode-supported Lipid Bilayer Membranes for In Vitro Cytochrome c Sensing," *Sensors Journal, IEEE*, 6(2):420–427.
- Luo, T.-J.M., Soong, R., Lan, E., Dunn, B. and Montemagno, C. 2005. "Photo-induced Proton Gradients and ATP Biosynthesis Produced by Vesicles Encapsulated in a Silica Matrix," *Nature Materials*, 4(3):220–224.
- Menestrina, G. 1986. "Ionic Channels Formed by Staphylococcus Aureus Alpha-Toxin: Voltage-dependent Inhibition by Divalent and Trivalent Cations," *Journal of Membrane Biology*, 90(2):177–190.
- Merzlyak, P.G., Capistrano, M.-F.P., Valeva, A., Kasianowicz, J.J. and Krasilnikov, O.V. 2005. "Conductance and Ion Selectivity of a Mesoscopic Protein Nanopore Probed with Cysteine Scanning Mutagenesis," *Biophysics Journal*, 89(5):3059–3070.
- Montal, M. and Mueller, P. 1972. "Formation of Bimolecular Membranes from Lipid Monolayers and a Study of their Electrical Properties," *Proceedings of the National Academy of Sciences*, 69(12):3561–3566.
- Mueller, P. and Rudin, D.O. 1963. "Induced Excitability in Reconstituted Cell Membrane Structure," *Journal of Theoretical Biology*, 4(3):268–280.

- Mueller, P., Rudin, D.O., Tien, H.T. and Wescott, W.C. 1962. "Reconstitution of Excitable Cell Membrane Structure In Vitro," *Circulation*, 26:1167–1171.
- Mueller, P., Rudin, D.O., Tien, H.T. and Wescott, W.C. (1964). "Formation and Properties of Bimolecular Lipid Membranes," *Recent Progress in Surface Science*, 1:379–393.
- Naumann, R., Baumgart, G.P.T., Jonczyk, O.A.A. and Knoll, W. 2002. "Proton Transport Through a Peptide-tethered Bilayer Lipid Membrane by the H<sup>+</sup>-ATP Synthase from Chloroplasts Measured by Impedance Spectroscopy," *Biosensors & Bioelectronics*, 17:25–34.
- Naumowicz, M., Petelska, A.D. and Figaszewski, Z.A. 2003. "Capacitance and Resistance of the Bilayer Membrane Formed of Phosphatidylcholine and Cholesterol," *Cellular & Molecular Biology Letters*, 8:5–18.
- Naumowicz, M., Petelska, A.D. and Figaszewski, Z.A. 2005. "Impedance Analysis of Phosphatidylcholine-Cholesterol System in Bilayer Lipid Membranes," *Electrochimica Acta*, 50:2155–2161.
- Needham, D. and Haydon, D.A. 1983. "Tensions and Free Energies of Formation of "Solventless" Lipid Bilayers. Measurement of High Contact Angles," *Biophysical Journal*, 41(3):251–257.
- Needham, D. and Hochmuth, R.M. 1989. "Electro-mechanical Permeabilization of Lipid Vesicles. Role of Membrane Tension and Compressibility," *Biophys. J.* 55(5):1001–1009.
- Nikolelis, D.P. and Siontorou, C.G. 1995. "Bilayer Lipid Membranes for Flow Injection Monitoring of Acetylcholine, Urea, and Penicillin," *Analytical Chemistry*, 67:936–944.
- Okazaki, T., Sakoh, M., Nagaoka, Y. and Asami, K. 2003. "Ion Channels of Alamethicin Dimer N-Terminally Linked by Disulfide Bond," *Biophysics Journal*, 85(1):267–273.
- Ottova, A. and Tien, H.T. 2002. "The 40th Anniversary of Bilayer Lipid Membrane Research," *Bioelectrochemistry*, 56:171–173.
- Ottova, A.L. and Ti Tien, H. 1997. "Self-assembled Bilayer Lipid Membranes: From Mimicking Biomembranes to Practical Applications," *Bioelectrochemistry and Bioenergetics*, 42(2):141–152.
- Reimhult, E. and Kumar, K. 2008. "Membrane Biosensor Platforms using Nano- and Microporous Supports," *Trends in Biotechnology*, 26(2):82–89.
- Requena, J., Billett, D.F. and Haydon, D.A. 1975. "Van Der Waals Forces in Oil-Water Systems from the Study of Thin Lipid Films. I. Measurement of the Contact Angle and the Estimation of the Van Der Waals Free Energy of Thinning of a Film," *Proceedings of the Royal Society of London. Series A, Mathematical and Physical Sciences (1934–1990)*, 347(1649):141–159.
- Robello, M. and Gliozzi, A. 1989. "Conductance Transition Induced by an Electric Field in Lipid Bilayers," *Biochimica et Biophysica Acta (BBA) – Biomembranes*, 982(1):173–176.
- Romer, W. and Steinem, C. 2004. "Impedance Analysis and Single-channel Recordings on Nano-Black Lipid Membranes Based on Porous Alumina," *Biophysics Journal*, 86(2):955–965.
- Rondelez, Y., Tresset, G., Nakashima, T., Kato-Yamada, Y., Fujita, H., Takeuchi, S. and Noji, H. 2005. "Highly Coupled ATP Synthesis By F1-ATPase Single Molecules," *Nature*, 433(7027):773–777.
- Sabo, J., Ottova, A., Laputkova, G., Legin, M., Vojcikova, L. and Tien, H.T. 1997. "A Combined AC-DC Method for Investigating Supported Bilayer Lipid Membranes," *Thin Solid Films*, 306:112–118.
- Sackmann, E. 1996. "Supported Membranes: Scientific and Practical Applications," *Science*, 271:43–48.
- Sarles, S. A., Sundaresan, V.B. and Leo, D.J. (2007). "Electrical Impedance Analysis of Phospholipid Bilayer Membranes for Enabling Engineering Design of Bio-Based Devices," In: *MRS Fall Meeting*, MRS, Boston, MA USA.
- Schmidt, C., Mayer, M. and Vogel, H. 2000. "A Chip-based Biosensor for the Functional Analysis of Single Ion Channels," *Angewandte Chemie International Edition*, 39(17):3137–3140.
- Song, L., Hobaugh, M.R., Shustak, C., Cheley, S., Bayle, H. and Gouaux, J.E. 1996. "Structure of Staphylococcal alpha-Hemolysin, a Heptameric Transmembrane Pore," *Science*, 274(5294):1859–1865.
- Sundaresan, V. B., Homison, C., Weiland, L.M. and Leo, D.J. 2007a. "Biological Transport Processes for Microhydraulic Actuation," *Sensors and Actuators B: Chemical*, 123(2):685–695.
- Sundaresan, V.B. and Leo, D.J. 2008. "Modeling and Characterization of a Chemomechanical Actuator using Protein Transporter," *Sensors and Actuators B: Chemical*, 131(2):384–393.
- Sundaresan, V.B., Sarles, S.A. and Leo, D.J. (2007b). "Chemoelectrical Energy Conversion of Adenosine Triphosphate," In: *Active and Passive Smart Structures and Integrated Systems 2007*, SPIE, San Diego, California, USA.
- Sundaresan, V.B., Sarles, S.A. and Leo, D.J. (2008). *Characterization of Porous Substrates for Biochemical Energy Conversion Devices*, SPIE, San Diego, CA.
- Thompson, M., Lennox, R.B. and McClelland, R.A. 1982. "Structure and Electrochemical Properties of Microfiltration Filter-Lipid Membrane Systems," *Analytical Chemistry*, 54:76–81.
- Tien, H.T. 1984. "Cyclic Voltammetry of Bilayer Lipid Membranes," *Journal of Physical Chemistry*, 88:3172–3174.
- Tien, H.T. and Ottova, A.L. 2001. "The Lipid Bilayer Concept and its Experimental Realization: From Soap Bubbles, Kitchen Sink, to Bilayer Lipid Membranes," *Journal of Membrane Science*, 189:83–117.
- Vodyanoy, I., Hall, J.E. and Balasubramanian, T.M. 1983. "Alamethicin-induced Current-Voltage Curve Asymmetry in Lipid Bilayers," *Biophysical Journal*, 42(1):71–82.
- Vodyanoy, I., Hall, J.E. and Vodyanoy, V. 1988. "Alamethicin Adsorption to a Planar Lipid Bilayer," *Biophysical Journal*, 53:649–658.
- Vriezema, D.M., Garcia, P.M.L., Oltra, N.S., Hatzakis, N.S., Kuiper, S.M., Nolte, R.J.M., Rowan, A.E. and van Hest, J.C.M. 2007. "Positional Assembly of Enzymes in Polymersome Nanoreactors for Cascade Reactions," *Angewandte Chemie International Edition*, 46(39):7378–7382.
- Wiegand, G., Arribas-Layton, N., Hillebrandt, H., Sackmann, E. and Wagner, P. 2002. "Electrical Properties of Supported Lipid Bilayer Membranes," *Journal of Physical Chemistry B*, 106:4245–4254.
- Wilburn, J. P., Wright, D.W. and Cliffel, D.E. 2006. "Imaging of Voltage-gated Alamethicin Pores in a Reconstituted Bilayer Lipid Membrane via Scanning Electrochemical Microscopy," *The Analyst*, 131(2): 311–316.
- Wong, D., Jeon, T.-J. and Schmidt, J. 2006. "Single Molecule Measurements of Channel Proteins Incorporated into Biomimetic Polymer Membranes," *Nanotechnology*, 17(15):3710.